Bifurcation of internal solitary wave modes from the essential spectrum

P. G. Kevrekidis[1] and C. K. R. T. Jones[2]
[1]*Department of Physics and Astronomy, Rutgers University, Piscataway, New Jersey 08854-8019*
[2]*Center for Fluid Mechanics, Brown University, Providence, Rhode Island 02912*
(Received 28 June 1999)

The bifurcation of internal modes from the phonon band in models supporting solitary wave solutions is currently one of the exciting phenomena in the field. We will present a number of analytical and semianalytical techniques for the detection, study, and understanding of these modes. We will see how they appear, without threshold, due to the discretization of the continuum equations. This perturbation is viewed in terms of a singular continuum approximation and analyzed by both perturbation theory and the Evans's function method. It is shown that these methods give equivalent results. Moreover, they are corroborated by mixed analytical-numerical computations based on the recently developed discrete Evans's function method. The extent to which these predictions survive to strong discretizations is discussed. The results will be presented in the context of both the sine-Gordon and the ϕ^4 models.

PACS number(s): 45.05.+x, 45.10.Hj, 63.20.Pw

I. INTRODUCTION

In the past few decades, solitary wave solutions have been recognized as a characteristic of many physical systems ranging from information transmission in Josephson junctions and optical fiber arrays [1–5] to the transcription of genetic material and the local denaturation of the base pair hydrogen bonds in the DNA double helix [6–10]. It has been recognized, however, that many of these applications (such as the Josephson junctions, the DNA problem, the motion of dislocations in solid state physics [11–13], or even the behavior of an array of coupled torsion pendula [14]) are inherently discrete in nature and thus necessitate that the problem be studied in the context of a lattice. Hence, in the past two decades, there has been a rapidly increasing number of papers that are concerned with the drastic modifications of the continuum solitary wave system behavior, once it is posed on a lattice. Very important contributions in identifying these traits were given by Peyrard and Kruskal [15] and Ishimori and Munakata [16] for the sine-Gordon equation and by Combs and Yip [17] for the ϕ^4 model.

In brief, the main changes that occur when studying models with Hamiltonian structure supporting solitary wave solutions on a discrete setup are the following:

(i) The breaking of translational invariance creates a nonzero Goldstone frequency which coupled to the phonons creates wave excitations radiating energy away from the coherent structure and, thus, contributing to its energy loss.

(ii) Also, all the configurations are no longer equivalent on the lattice but there is a maximum (kink centered on a site) and a minimum (kink centered between sites) energy configuration leading to the creation of a barrier analogous to the one dislocations have to overcome in order to propagate on a lattice, and hence is termed the Peierls-Nabarro (PN) barrier.

(iii) Due to the resonances, the gradual kinetic energy loss leads to trapping of the kink in one of the PN barriers between two lattice sites. It, thereafter, executes a nonlinearly damped oscillation in that potential barrier until it reaches an asymtotically stable state [18].

However, even though there was a series of papers that elaborated on and clarified the above issues (i.e., the resonances [18,19], the PN oscillation [18–20], the stability of coherent solitonlike structures on diffusively coupled lattices [21], as well as the collective variable behavior of these structures [22–26]), not all of the story was unveiled. In particular, Braun, Peyrard, and Kivshar observed much later [27] that in a range of parameter values for the discrete sine-Gordon equation (also known as the Frenkel-Kontorova model and originally proposed for the study of dislocations [11]), a discrete mode bifurcated from the bottom edge of the phonon spectrum. Both mathematically and physically the study of this bifurcation is an important problem—mathematically because one can develop techniques to quantitatively predict when this bifurcation will occur and what its magnitude will be, and physically because this internal mode will create oscillations that will modify the shape of the transmitted information (i.e., in the array of coupled Josephson junctions). Therefore, one would be interested in finding out what the form of this shaping factor will be (and thus its effect on the transmitted bits or kinks) and when it will appear.

One important subsequent paper of Kivshar *et al.* [28] revealed the characteristic that the birth of these internal modes is thresholdless (i.e., the mode appears as soon as the continuum problem is set on a lattice). These authors also gave a quantitative method of prediction of the magnitude of these bifurcations based on singular perturbation theory.

Our aim in this paper will be twofold:

(1) For two important models that support solitonlike solutions, namely the discrete sine-Gordon and ϕ^4 models, we will first study discreteness as a perturbation of the continuum through the singular perturbation theory proposed in [28] and through the Evans function as proposed in [29,30]. We will show the equivalence of the two approaches for this problem and will quantify their predictions.

(2) On the other hand, using linear stability analysis and a semianalytical methodology introduced in [21], the discrete Evans function technique, we will trace the exact bifurcation

of the discrete internal mode from the phonon band and will indicate where (and why) the semicontinuum methods will break down. We will refer to the singular perturbation methods or the continuum Evans technique as semicontinuum approaches since they are attempting to approximate the effects of discreteness by a singular (higher-order derivative) perturbation of the continuum problem. Such methodologies should be anticipated to work well close to the continuum limit (for weak discreteness). They should also, however, be expected to break down for strong discreteness. The reason for that is that many of the inherently discrete phenomena (such as the breaking of translational invariance and the nonzero Goldstone frequency or the nonequivalence of configurations and the PN barrier) are not captured by such singular continuumlike perturbations.

In this way, we hope to provide a comprehensive set of tools and of results pertinent to this problem in order to reveal the main characteristics and the physical aspects of behavior of these solitary wave modes.

Our presentation will be organized as follows: In Sec. II we will follow the approach of [28] in presenting the singular perturbation methodology. In Sec. III the continuum Evans function approach will be presented and the equivalence of its results to the ones of Sec. II will be established. In Sec. IV, the discrete Evans technique will be introduced and implemented. Its results will be compared to the linear stability analysis and to the semicontinuum perturbation methods. Finally, in Sec. V, a summary of the results and conclusions as well as an outlook of potential extensions of this work will be outlined.

II. PERTURBATION THEORY

Let us consider the case of the sine-Gordon equation treating discreteness as a perturbation. Following the notation of [28] we can write it as

$$u_{tt}=u_{xx}-\sin u+\epsilon g(u), \tag{1}$$

where $\epsilon=h^2/12$ and $g(u)=u_{xxxx}$ if we consider only the fourth derivative [i.e., the first-order perturbation in the Taylor expansion: $(u_{i+1}+u_{i-1}-2u_i)/h^2=\Sigma_{j=1}(2h^{2j-2}/2j!)(\partial^{2j}u/\partial x^{2j})$].

The expression of the perturbation can be suitably modified if higher-order terms are included. Expressing the solution as a perturbation series [using ϵ as a perturbation (control) parameter] $u=u^0+\epsilon u^1+\cdots$ one can explicitly derive the equation that u^1 satisfies,

$$u^1_{xx}-\cos u^0 u^1=g(u^0), \tag{2}$$

and find the solution to be

$$u^1(x)=\frac{1}{\cosh x}\int_{-\infty}^{x}dx'\cosh^2 x'\int_{-\infty}^{x'}dx''\frac{g(u^0)}{\cosh x''}. \tag{3}$$

It is important here to make the observation that the lower limit of our integration is $-\infty$ as opposed to 0 as appears in [28]. For the case of the sine-Gordon with the fourth- and/or higher-order derivative perturbation explicit calculations can show that the integral with a zero lower bound yields a divergence [as the astute reader can readily realize viewing the lower bound of the innermost integral's integrand as a constant and seeing the divergence arise from $(1/\cosh x)\int^x dx'\cosh^2 x'$]. Thus, this substitution is necessary in order to avoid any unphysical divergences.

Linearization around the perturbed kink using

$$u(x,t)=u^0+\epsilon u^1+w(x)\exp(i\omega t) \tag{4}$$

yields the perturbed eigenvalue problem

$$-\omega^2 w=w_{xx}+\left(\frac{2}{\cosh^2 x}-1\right)w+\epsilon u^1\sin u^0 w. \tag{5}$$

The spectrum of the unperturbed fully integrable continuum sine-Gordon model [31] consists of (i) a Goldstone eigenmode with zero frequency and the even spatial structure of the kink spatial derivative, $W_G(x)=u^0{}_x$ and (ii) a semiinfinite continuum band of phonons that satisfies the dispersion relation $\omega^2=1+k^2$. The corresponding wave functions for each k are $W(x,k)=\exp(ikx)[(k+i\tanh x)/(k+i)]$. The lower edge of the band $(k=0)$ has $\omega_{edge}=1/d$ and a nonsecularly growing hyperbolic tangent eigenfunction profile.

One can now take advantage of the fact that this is a complete (basis) set of eigenfunctions to express the perturbed eigenfunctions of Eq. (5) using their projection on this basis set. Thus one can write

$$w(x)=a_G W_G+\int a(k)W(x,k)dk. \tag{6}$$

Back substitution in Eq. (5)—neglecting the irrelevant contribution of the Goldstone projection—yields

$$a(k)=\frac{\epsilon}{2\pi}\int_{-\infty}^{\infty}\frac{K(k,k')a(k')}{k'^2+\epsilon^2 b^2}dk', \tag{7}$$

where

$$K(k,k')=\int W^{\star}(x,k)u^1\sin u^0 W(x,k')dk' \tag{8}$$

is a Fourier space integral kernel and the bifurcating eigenvalue has been assumed to have a frequency $\omega_{bif}{}^2=1-\epsilon^2 b^2$. Notice that we have specifically used Eq. (6) in Eq. (5) for the bifurcating mode (seeking its spatial profile), hence the substitution of the relevant frequency.

The authors of [28] extracted the singular contribution to the integral by setting $k'=0$ in the numerator and integrating over the Lorentzian curve. In this way they obtained

$$a(k)=\frac{\mathrm{sgn}(\epsilon)}{2|b|}K(k,0)a(0). \tag{9}$$

However, for $k=0$ (i.e., the phonon band edge) Eq. (9) imposes a solvability condition for the detuning parameter ϵb, namely,

$$|\epsilon b|=\frac{1}{2}\epsilon\int_{-\infty}^{\infty}\tanh^2 x u^1\sin u^0 dx, \tag{10}$$

Up to now, we have briefly reproduced the arguments given in [28]. Even though some of the details may be deemed as unnecessary as the full presentation is given in [28], we believe that in view of the establishment of the equivalence of the results of the method with the continuum Evans function technique, their presentation is useful. In addition, our pedagogic aim of presenting a reference paper that encompasses all the methodologies and techniques used to date for such problems, we believe, justifies such an exposition.

For the case of the sine-Gordon model, we have studied not only the case of quartic but also of sixth- and higher-order perturbations and we give the full results below. In the case of the quartic one, the functional form of u^1 can be explicitly found to be

$$u^1(x)=\left(-3+\frac{6+x+\exp(2x)x}{1+\exp(2x)}\right)\Big/\cosh x. \tag{11}$$

We will give the parametric dependence of the results for both models in accordance with their form as it appears in the standard reference on the subject ([15]). The discrete lattice equations of the Frenkel-Kontorova model are then

$$u_{i,tt}=u_{i+1}+u_{i-1}-2u_i-\frac{1}{d^2}\sin u_i \tag{12}$$

and, using the appropriate rescaling $h\to 1/d$, $\omega\to d\omega$, the detuning parameter of the discrete mode will be (up to second-order perturbative corrections)

$$\epsilon b=\frac{1}{2}\left(\frac{0.088\,888\,89}{d^2}-\frac{0.004\,761\,9}{d^4}\right). \tag{13}$$

Higher orders can be seen to saturate to this order of correction to a very good degree of approximation. The discrete mode then detaching from the bottom edge ($\omega_{edge}=1/d$) of the phonon band will have a frequency ${\omega_{bif}}^2=(1/d^2)(1-\epsilon^2 b^2)$. Similarly, the discrete ϕ^4 model assumes the form

$$u_{i,tt}=u_{i+1}+u_{i-1}-2u_i+\frac{1}{d^2}(u_i-u_i^3) \tag{14}$$

and again by using the appropriate rescaling, $h^2\to 1/(2d^2)$, $\omega\to\sqrt{2}\,d\omega$, of the notation of [28], one finds that the bifurcating frequency will be

$${\omega_{bif}}^2=\frac{2}{d^2}\left(1-\frac{1}{15^2 d^4}\right) \tag{15}$$

away from the bottom edge ($\omega_{edge}=\sqrt{2}/d$) of the essential spectrum (to first order which, as claimed in [28], gives an excellent approximation to the numerical predictions. The accuracy of this statement will be examined later). We have, so far, reformulated (making some minor modifications) and presented the methodology of [27,28] in identifying and quantifying the bifurcation of discrete modes from the bottom edge of the essential spectrum. We have also applied this methodology to the discrete sine-Gordon and ϕ^4 models. Let us now present an alternative approach as given in the context of the perturbed nonlinear Schrödinger equation in [29,30] that will complement this presentation yielding an equivalent formulation.

III. CONTINUUM EVANS FUNCTION

First, we give the basic idea behind the Evans function method. The eigenvalue problem around the continuum kink has a subspace of solutions that decay for large positive x, E^s. It also contains a subspace of solutions that decay for large negative x, E^u. If there exists a frequency ω for which these two subspaces intersect (i.e., a frequency for which their wedge product, defined to be the Evans function: $E(\omega)=E^u\wedge E^s$, vanishes) then, by construction, that ω is an eigenvalue which corresponds to a localized eigenfunction. Thus, the Evans function is a function whose zeros yield the discrete modes pertaining to the coherent structure sustained by the model under study. Coming back to our example, the eigenvalue problem can be written (using notation in accordance to [29]) as

$$Y'=M(x,\omega,\epsilon)Y \tag{16}$$

where the matrix M is

$$M=\begin{bmatrix}0 & 1\\ g(x)-\omega^2 & 0\end{bmatrix} \tag{17}$$

and $g(x)=1-(2/\cosh^2 x)-\epsilon u^1\sin u^0$ as can be seen from the preceding section. Setting

$$M_0=\lim_{|x|\to\infty} M(\omega,x,0),$$

the eigenvalues of this limit matrix are $\pm\gamma$ where $\gamma=-ik=\sqrt{|\omega^2-1|}\exp[i/2\arg(1-\omega^2)]$ for $\arg(1-\omega^2)\in[-\pi/2,3\pi/2)$ (the details of why we consider the branch cuts can be found in [29] but will also be clear later on). The corresponding eigenfunctions are $[1,\pm\gamma]$.

In our case, however, we also know [31,28] (both in the sine-Gordon and ϕ^4 cases) the full scattering operator eigenspectrum and the corresponding set of eigenfunctions. In the sine-Gordon (SG) case the forward eigenfunctions that decay for large positive x are

$$Y^+=\begin{bmatrix}P(\gamma,x)\\ Q(\gamma,x)\end{bmatrix}, \tag{18}$$

where $P(\gamma,x)=\exp(-\gamma x)[(\gamma+\tanh x)/(\gamma+1)]$ and $Q=P'$. On the other hand, the solutions exponentially decaying far to the left of the kink ($x\to-\infty$) are

$$Y^-=\begin{bmatrix}P(\gamma,-x)\\ -Q(\gamma,-x)\end{bmatrix}, \tag{19}$$

where P,Q again is as defined above. Furthermore, it is straightforward to verify that the adjoint problem $Z'=-M^T Z$ has solutions (that will be used in what follows) $Z=[-Q(\omega,x),P(\omega,x)]^T$. One can verify the following limit relations [analogous to Eq. (3.5) of [29]]:

$$\lim_{x\to\mp\infty} Y^-\exp(\mp\gamma x)=[1,\pm\gamma]^T$$

and

$$\lim_{x\to\pm\infty} Y^{-}\exp(\mp\gamma x)=\frac{\gamma-1}{\gamma+1}[1,\pm\gamma]^{T}.$$

Then, using the above definition of the Evans function: $E(\omega)=Y^{-}\wedge Y^{+}$, one finds

$$E=2\gamma\left(1-\frac{2\gamma}{1+\gamma}\right) \tag{20}$$

that can be written as (see remark 4.3 in [29])

$$E=2\gamma[1+g_2(\omega)] \tag{21}$$

with g_2 continuous and vanishing at the bottom edge of the phonon band. On the other hand, according to Theorem 4.2 of [29] (see also [32]) the derivative of the Evans function evaluated at the bottom edge of the phonon band is

$$\partial E_{\epsilon}(1/d,\epsilon=0)=\int_{-\infty}^{\infty} Z(1/d,x,0)\partial M_{\epsilon}(1/d,x,0)Y^{+}(1/d,x,0)dx \tag{22}$$

(where as usual the subscript denotes partial derivative with respect to the subscript variable). In the sine-Gordon case

$$\partial E_{\epsilon}(1/d,\epsilon=0)=-\int_{-\infty}^{\infty}\tanh^{2}xu^{1}\sin(u^{0})dx, \tag{23}$$

an expression which is certainly familiar from the presentation in Sec. II. Now by using the differentiability of the Evans function to expand it in a Taylor series around the bottom edge of the essential spectrum, we get $E(\omega,\epsilon)=E(\omega,0)+[\partial E_{\epsilon}(1/d,\epsilon=0)+g_1(\omega,\epsilon)]\epsilon$, where g_1 is also continuous and vanishing at $\omega_{edge}=1/d$. Then, if the argument of the derivative does not belong in the domain $(-\pi/4,3\pi/4)$ (due to the branch cuts taken above), then there is no bifurcation. In our case this statement translates to $\mathrm{sgn}(\epsilon)\int_{-\infty}^{\infty}\tanh^{2}(x)u^{1}\sin(u^{0})dx$ being negative. But in that case, the right-hand side of Eq. (10) would be negative and the solvability condition of [28] would not be satisfied. Hence, no bifurcation would occur. On the other hand, if the quantity above is positive then the vanishing of $E(\omega,\epsilon)$ will occur according to the expansion at ${\omega_{bif}}^{2}=(1/d^{2})(1-\epsilon^{2}b^{2})$, where ϵb is defined exactly as in the perturbation theory treatment. Therefore, the two approaches are shown to yield the exact same result for the bifurcation of the discrete mode from the bottom edge of the continuum spectrum of the sine-Gordon equation. Furthermore, since the condition is satisfied for the appearance of the mode (as the predictions made in Sec. II indicate) for any d, the discrete mode should (according to these predictions) be present for all d as soon as one studies the problem on the lattice (hence, its generation is thresholdless). The proof is exactly the same in the case of the ϕ^4 model and will be left to the reader as an interesting exercise. The only thing that changes is the form of the unperturbed spectrum and the form of the perturbation that is dependent on the nonlinearity. Otherwise, the verification of the equivalence of the two methods can follow the exact same path.

It is perhaps not surprising that the two methods render the same answer. The derivative of the Evans function is known to be equivalent to a Melnikov function, see [33,34]. It is also well known that Melnikov calculations can be derived in an alternative way using a solvability condition, see [35]. The singular perturbation theory approach used above fits into this framework and thus the equivalence of the results coming from the two methods is based on the equivalence of the two methods as the two different approaches to the Melnikov method.

Having presented the two approaches that treat discreteness as a perturbation, we will now give a semianalytical method that corresponds to the discrete version of the Evans function technique and which appeared in [21]. Its results will then be compared to those of the above methods and to the ones from linear stability analysis and the differences will be highlighted and explained.

IV. SEMIANALYTICAL METHODS AND COMPARISON

A. Linear stability analysis and the discrete Evans function

Let us now return to the fully discrete problem. In order to construct a discrete eigenfunction one must find a solution that decays to the left as well as to the right far away from the coherent structure. The uniform steady states approached (exponentially) far to the left and far to the right of the kink are $u=0$, $u=2\pi$, respectively (-1 and 1 for the ϕ^4). The linearized equation around the coherent structure will read

$$\omega^{2}y_i=y_{i+1}+y_{i-1}-2y_i-\frac{1}{d^{2}}\cos u_i y_i \tag{24}$$

in the SG model and

$$\omega^{2}y_i=y_{i+1}+y_{i-1}-2y_i-\frac{1}{d^{2}}(3u_i^{2}-1)y_i \tag{25}$$

in ϕ^4 (where $\{u_i\}$ is the profile of the exact discrete static kink).

In order to trace the discrete eigenvalues, the most simple numerical method is to solve the full eigenvalue problem as follows.

(i) One can construct the exact discrete kink, through a Newton-Raphson iteration, solving the system of equations

$$u_{i+1}+u_{i-1}-2u_i-\frac{1}{d^{2}}\sin u_i=0 \tag{26}$$

(analogously defined for ϕ^4) with a continuum kink initial condition.

(ii) Using the exact discrete kink $\{u_i\}$, one can then solve the matrix eigenvalue problems of Eqs. (24) and (25) to find the eigenfunctions and eigenvalues in the framework of linear stability analysis.

This methodology will yield both the localized modes as well as the extended phonon modes.

On the other hand, if one is interested in the localized (internal soliton) modes only, one has to construct a decaying solution far away from the kink, on either side of the lattice. The linearized equation is simplified far away from the kink since $\cos u_i \to 1$ and $3u_i^2 - 1 \to 2$. Thus Eqs. (24) and (25) become constant coefficient second-order difference equations whose solutions are of the form

$$y_i = C_{\pm}(\omega) r_1^i + D_{\pm}(\omega) r_2^i, \tag{27}$$

with

$$r_{2,1} = \frac{1}{2}[\omega^2 + 2 + \omega_{edge}^2 \pm \sqrt{(\omega^2 + \omega_{edge}^2)(\omega^2 + \omega_{edge}^2 + 4)}]. \tag{28}$$

Let us point out that the only difference in Eq. (28) between the two models under study (SG, ϕ^4) will be their different ω_{edge} $(1/d, \sqrt{2}/d$, respectively).

Then, constructing a perturbation that decays as $u_i = D_- r_2^i$ (which has the proper exponential decay behavior) as $i \to -\infty$ and shooting through the kink [using Eqs. (24) and (25)], a solution with both decaying and growing parts is obtained far to the right, i.e.,

$$y_i = C_+ r_1^i + D_+ r_2^i. \tag{29}$$

D_+ pertains to the growing part. Hence, if a frequency is found such that the prefactor of the growing part, $D_+(\omega)$, vanishes, then this frequency corresponds to a mode that decays on both sides of the coherent structure and is, thus, a localized eigenfunction.

For a lattice that extends up to $i = L+1$, using Eq. (29) for sites $i = L-1, L, L+1$, one obtains

$$D_+(\omega) = \frac{y_{L+1} - r_1 y_L}{r_2^{L+1} - r_2^L r_1} = \frac{r_2 y_L - y_{L-1}}{r_2^{L-1}(r_2^2 - 1)}. \tag{30}$$

For technical (normalization) reasons explained in [21], it is (numerically) convenient to start on the left side with $D_-(\omega) = r_1^{2L}$ (where L is the size of our lattice) and also to remove the branch cuts introduced from the edges of the phonon band ($r_2^2 = 1$). This is done by rescaling Eq. (30) by multiplying with $(r_2^2 - 1)/r_2^2$ [21]. We *define* this rescaled version of the transmission coefficient of Eq. (30) as the discrete Evans function. Clearly, in correspondence with the continuum construction, the zeros of the discrete Evans function [which can be found numerically by implementing the shooting process mentioned above and using Eq. (30)], will provide the localized eigenmode frequencies.

B. Results and comparison

Having set up all the methods relevant to the problem of the internal shape mode bifurcations from the essential spectrum, let us now present their results for the two discrete models of concern to this study. Linear stability analysis shows that (i) in the discrete sine-Gordon model (Fig. 1), the spectrum consists of the following:

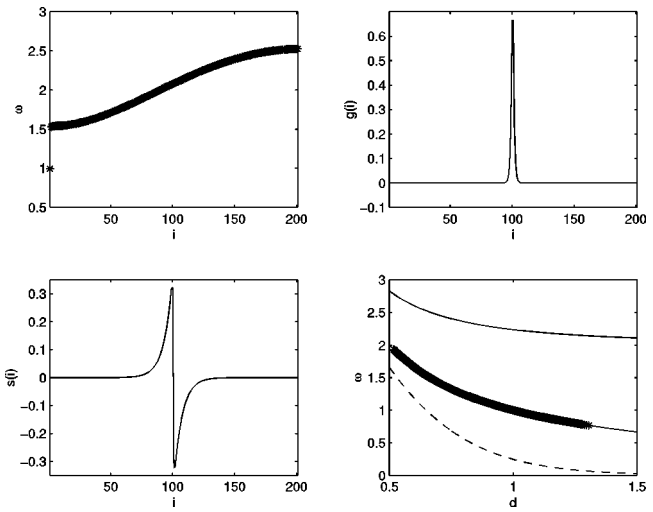

FIG. 1. Spectrum of linearization around a discrete static sine-Gordon kink for $d = 0.7$. Upper left: full linearization frequency spectrum around the exact discrete stable static kink for a 200 site lattice. Upper right: Goldstone mode spatial profile; bottom left: internal mode spatial profile. Bottom right: Behavior of the linearization spectrum frequencies as a function of d. The dashed line shows ω_G as a function of d, the thick line shows ω_{bif} as a function of d, whereas the two solid lines indicate the lower and upper edge of the phonon band $(1/d, \sqrt{4 + (1/d^2)}$, respectively)—linear stability analysis results.

(1) A discrete Goldstone mode which, due to the breaking of the translational invariance has a nonzero frequency.

(2) A band of extended waves (phonons) that satisfy the dispersion relation $\omega^2 = 2 - 2\cos k + 1/d^2$. From this equation, it can be seen that the band has frequencies only in the interval $[1/d, \sqrt{4 + (1/d^2)}]$ (rather than being semi-infinite as in the continuum problem).

(3) In addition to the above frequencies, for $d \geqslant 0.515$ a shape mode bifurcates from the bottom of the phonon band. The dependence of the ''distance'' $(\omega_{edge} - \omega_{bif})$ of this mode's frequency from the band edge is shown in Fig. 2. One can see that after a maximum excursion (the maximum occurring for $d \approx 0.7$), the frequency of the mode approaches the band edge frequency as d increases. Eventually, its distance from the edge becomes of the order of 10^{-5} for $d \approx 1.3$ and gradually as its frequency comes very close to the one of the band edge, the spatial profile of the mode becomes extended covering all of the lattice. For larger lattices this occurs for larger d and for the infinite lattice (presumably) the degeneration occurs for $d \approx \infty$ justifying the conclusion of the thresholdless birth of this solitary wave internal eigenmode.

(ii) In the ϕ^4 case, the continuum contains already two localized eigenmodes: the zero frequency Goldstone and an odd eigenmode of frequency $\sqrt{3/2d^2}$. In the discrete case we find (Fig. 3) the following:

(1) A nonzero frequency G mode due to the breaking of translational invariance.

(2) The counterpart of the second continuum localized mode.

(3) A finite band of phonon frequencies [according to the dispersion relation $\omega^2 = 2 - 2\cos k + (2/d^2)$] which extends from $\omega_{edge} = \sqrt{2}/d$ to $\omega_{max} = \sqrt{4 + 2/d^2}$.

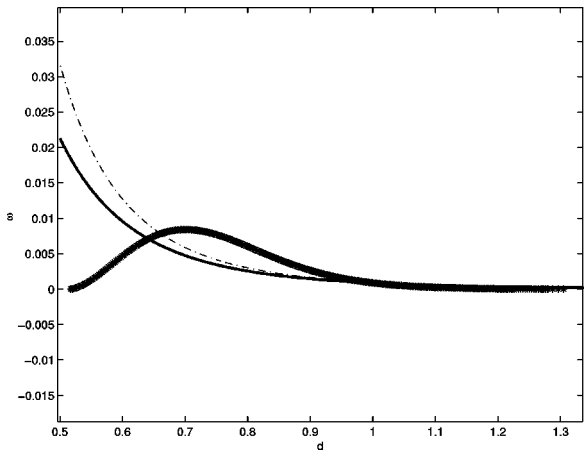

FIG. 2. Bifurcation of the internal mode in SG vs the discreteness parameter d: the solid line shows the (equivalent) continuum Evans and singular perturbation results for $\omega=\omega_{edge}-\omega_{bif}$ as a function of d for the quartic perturbation correction; the dash-dot line shows the same as before but for the fourth plus sixth derivative perturbation. The thick line of stars shows the discrete Evans function and linear stability results for the behavior of the same quantity as a function of the discreteness parameter (also see the text).

(4) And finally a localized eigenmode bifurcating from the edge of the continuum band for $d\geqslant 0.82$. The behavior of this internal mode is shown in Fig. 4 where its behavior can be seen to be similar to the one of its SG counterpart. In particular, after a maximal excursion (maximum occuring around $d\approx 1.05$) of its frequency away from the band edge frequency, ω_{bif} approaches ω_{edge} as d increases and eventually merges with the band edge as $d\to\infty$ (the continuum limit).

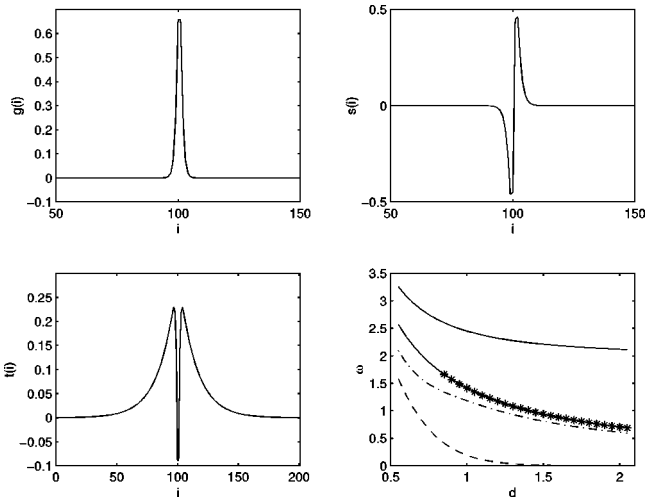

FIG. 3. Spectrum of linearization around an exact discrete static ϕ^4 kink for $d=1.0$. Upper left: Goldstone mode spatial profile; upper right: second localized mode spatial profile (see text); bottom left: internal bifurcating mode spatial profile; bottom right: parametric dependence of the linear stability spectrum as a function of the discreteness parameter d. The dashed line shows ω_G as a function of d; the dash-dot line indicates the dependence of the second localized mode frequency on the discreteness parameter; the stars represent $\omega_{bif}=\omega_{bif}(d)$, and once again the solid lines define the finite edge of phonons ($[\sqrt{2}/d, \sqrt{4+(2/d^2)}]$)—linear stability results.

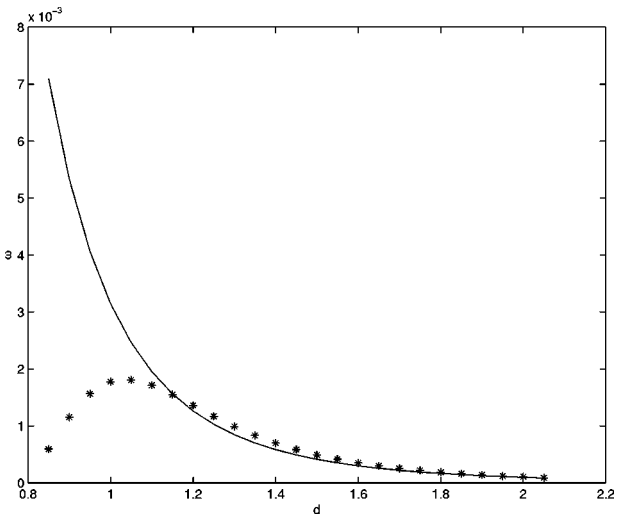

FIG. 4. Same as Fig. 2 but for the ϕ^4 model. The solid line shows the prediction for the bifurcation (i.e., $\omega=\omega_{edge}-\omega_{bif}$) of the internal mode as a function of d from semicontinuum theories. The stars indicate the actual behavior of the same quantity as given by semianalytical and/or numerical techniques (see text).

The results of the discrete Evans function technique and of linear stability analysis in Figs. 2 and 4 for the ''distance'' of the mode from the band edge are shown by the symbols. The solid and dash-dot lines demonstrate the (equivalent) predictions of semicontinuum theories for quartic and quartic plus sixth-order derivative perturbations, respectively. It is noteworthy that the results of linear stability and of the discrete Evans method coincide for the range of d values that are shown. For larger values of d, as our results indicate and as was found also in [21], the linear stability analysis becomes less accurate than the discrete Evans method due to finite size effects. Thus, the discrete Evans technique is the most accurate diagnostic of the discrete modes and of their bifurcation from the essential spectrum. The discrete Evans method results have been constructed by identifying the zeros of the Evans function for frequencies lying on the imaginary spectral plane axis (where the shape mode eigenfrequency has to lie, due to the Hamiltonian nature of the system). Moreover, in [21] the value of the Evans function at the bottom of the band edge $D_+(\omega=\omega_{edge})$ was used to probe internal mode bifurcations. The authors of [21] noticed that the change of sign of this value from negative to positive indicated the detachment of the internal mode from the edge. One can easily see that the equation $E(\omega_{edge},\epsilon)=\epsilon\partial_\epsilon E$ (for the perturbed Evans function at $\omega=\omega_{edge}$), together with Eqs. (22) and (10) prove the correctness of the above observation, i.e., the solvability condition is satisfied and the mode bifurcates when the value of the perturbed Evans function at the band edge changes sign.

On the other hand, viewing the predictions of the semicontinuum theories that treat discreteness as a perturbation, we realize that their predictions are quite successful close to the continuum limit (i.e., for large d). As d decreases, however, their prediction follows the one of the semianalytical and/or numerical methods down to $d\approx 0.9$ in the SG model and $d\approx 1.2$ in the ϕ^4 case. For lower values of the discrete-

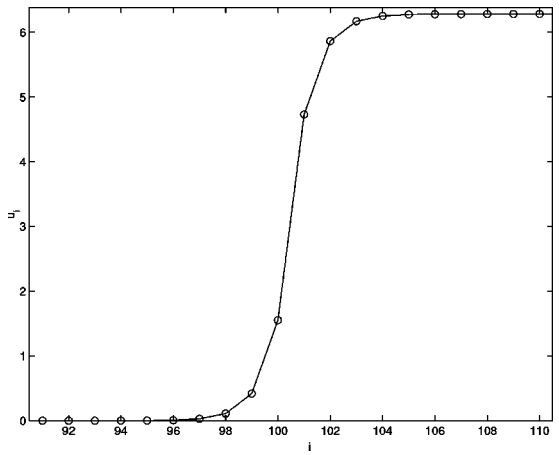

FIG. 5. Spatial profile of an exact discrete stable static 200-site kink for $d=0.7$. Shown are the displacement ordinates u_i as a function of the lattice site index i.

ness parameter (strong discreteness) the perturbative treatments do not accurately predict the behavior of the frequency of the bifurcating mode. It is well known from previous attempts to treat discreteness as a perturbation (such as [16], where the Keener-McLaughlin and McLaughlin-Scott [36,37] singular perturbation schemes were used to treat discreteness), that such methods cannot account for the results of very strong discreteness. As was mentioned also in the Introduction, this is due to the fact that many of the important phenomena (the PN barrier or the bifurcation of the G mode) are not captured by treating discreteness merely as a perturbation. Hence, the discrepancy between the semicontinuum predictions and the actual behavior of the internal wave mode frequency is to be anticipated.

However, one can go a step further in qualitatively explaining the behavior of the bifurcation frequency. In particular, as d decreases, by observing the structure of the exact discrete kink (see, i.e., Fig. 5), one notices that fewer lattice site ordinates ''participate'' in the ''spine'' of the kink. For example, in the SG, for $d<1$, practically only six sites contribute to the kink structure with ordinates symmetrically placed around π (i.e., $u_{i+1}=2\pi-u_{6-i}$, for $i=0,1,2$). In addition, only one of the three ordinates which have value less than π has $u_i>\pi/2$. This ordinate falls below $\pi/2$ after $d=0.7$. This can be very accurately also predicted by the approximate equations for a six-site kink, i.e., a kink with the approximate structure $(0,\ldots,0,a,b,c,2\pi-c,2\pi-b,2\pi-a,2\pi,\ldots,2\pi)$ in the SG case. These approximate equations (approximate because the ordinates before the first and after the sixth site are set to $0,2\pi$, respectively) read

$$b-2a-\frac{1}{d^2}\sin a=0, \tag{31}$$

$$c+a-2b-\frac{1}{d^2}\sin b=0, \tag{32}$$

$$b+2\pi-3c-\frac{1}{d^2}\sin c=0, \tag{33}$$

and predict a solution with $c<\pi/2$ for $d<0.707$. When this occurs, the sign of $\cos c$ in the linearized equations

$$y_{i+1}+y_{i-1}-2y_i-\frac{1}{d^2}\cos u_i y_i=-\omega^2 y_i \tag{34}$$

will change (and practically all other cosine terms will be ≈ 1) and thus in order to maintain the functional form and parity of the mode the solution changes sign $y_i\rightarrow -y_i$ as linear stability analysis verifies. As d decreases further, only four and then two sites contribute to the kink [for instance, for $d=0.3$ the kink practically consists of two sites and these have $\cos a=\cos(2\pi-a)\approx 0.9$].

Thus, Eq. (34) approaches (for decreasing d) the linearized equation around uniform steady states. The latter has extended wave solutions rather than localized internal eigenmodes. The limit of $d=0$ will, of course, find all sites to the left of the kink at the $u=0$ steady state whereas to the right at $u=2\pi$ (at $-1,+1$, respectively, for ϕ^4). Hence, it is the fact that the kink on the lattice consists of only few sites with ordinates differing from the uniform steady state, which causes the internal mode to bifurcate maximally and then gradually degenerate for very small d to an extended excitation and eventually disappear, in contrast to the semicontinuum theory results. The latter, treating discreteness as a continuumlike perturbation, always sees the kink as a translationally invariant structure with a spine that consists of infinite points. Thus, the semicontinuum theory predictions fail to capture the fact that as the lattice becomes more and more discrete the kink is less and less densely populated until in the end the linearized equation matches one of the phonon eigenmodes that satisfy the linear wave dispersion relation. This argument, we believe, highlights the point of difference between the semianalytical and/or numerical techniques and the semicontinuum theoretical predictions.

V. CONCLUSIONS AND FUTURE CHALLENGES

The scope of this paper has been threefold.

(1) Firstly, to present the semicontinuum methods, such as singular perturbation theory and the continuum Evans function technique, that approach the problem of the internal mode bifurcation. Discreteness is viewed in each approach as a perturbation and we have demonstrated the equivalence of their results.

(2) Secondly, to expose the semianalytical and numerical methods that one can use to identify these modes and the magnitude of their frequency bifurcation from the bottom edge of the essential spectrum. Linear stability analysis and the discrete Evans function were used in that direction and the near coincidence of their (numerical) results was demonstrated.

(3) Finally, the continuumlike methods were compared to the numerical results and the regimes in which their predictions agreed with the numerical experiments were indicated. Also highlighted was the breakdown of these techniques for highly discrete regimes as well as the reason for that breakdown (the sparsely populated spine of the discrete kinklike structure). In that context the qualitative picture of the internal mode behavior, as produced by the numerical simulations, was justified by means of simple physical arguments.

In conclusion, we have used a combination of available techniques and tools to study the two models of interest, the

SG and ϕ^4 discrete model equations, the thresholdless generation of an internal mode pertaining to the kink solitary wave due to discreteness. The smooth maximization of the bifurcation and the vanishing of the mode for strongly discrete lattices were numerically indicated and the disparity of this prediction from the one of perturbative treatments clarified.

An interesting extension of this study would involve an attempt to create a rigorous perturbative technique with which one could predict the mode frequency behavior in the highly discrete (small d) versions of the lattice models. This challenging theoretical task will be left for future studies.

ACKNOWLEDGMENTS

Thanks are expressed to M. I. Weinstein and Y. G. Kevrekidis for useful discussions and to N. J. Balmforth for assistance in the numerical component of this work. P.G.K. gratefully acknowledges support from a DIMACS award as well as financial support from the ''Alexander S. Onasis'' Public Benefit Foundation and the Computational Chemodynamics Laboratory. The research of C.K.R.T.J. was supported by the National Science Foundation under Grant No. DMS-9704906.

[1] A.V. Ustinov, T. Doderer, I.V. Vernik, N.F. Pedersen, R.P. Huebener, and V.A. Oboznov, Physica D **68**, 41 (1994).
[2] T. Holst, L.E. Guettero, N. Gronbech-Jensen, J.A. Blackburn, and J. Bindlev-Hansen, *Superconducting Devices and their Applications* (Springer-Verlag, Berlin, 1992).
[3] K. Xu, D. Lu, and X. Yao, Chin. J. Low Temp. Phys. **14**, 293 (1992).
[4] J. Kutz, C. Hile, W. Kath, R.-D. Li, and P. Kummar, J. Opt. Soc. Am. B **11**, 2112 (1994).
[5] J. Kutz, C. Hile, W. Kath, R.-D. Li, and P. Kummar, Opt. Lett. **18**, 802 (1993).
[6] M. Peyrard and A.R. Bishop, Phys. Rev. Lett. **62**, 2755 (1989).
[7] T. Dauxois, Phys. Lett. A **159**, 390 (1991).
[8] T. Dauxois, M. Peyrard, and C.R. Willis, Physica D **57**, 267 (1992).
[9] T. Dauxois, M. Peyrard, and A.R. Bishop, Physica D **66**, 35 (1993).
[10] X. Yang, Y. Zhuo, and X. Wu, Phys. Lett. A **234**, 152 (1997).
[11] J. Frenkel and T. Kontorova, J. Phys. USSR **1**, 137 (1939).
[12] J.H. Heiner, Phys. Rev. A **136**, 863 (1964).
[13] W. Atkinson and N. Cabrera, Phys. Rev. A **138**, 763 (1965).
[14] D.E. Pelinovsky and S.Kh. Shavratsky, Physica D **1**, 317 (1980).
[15] M. Peyrard and M.D. Kruskal, Physica D **14**, 88 (1984).
[16] Y. Ishimori and T. Munakata, J. Phys. Soc. Jpn. **51**, 3367 (1982).
[17] J.A. Combs and S. Yip, Phys. Rev. B **28**, 6873 (1983).
[18] P.G. Kevrekidis and M.I. Weinstein (unpublished).
[19] R. Boesch, C.R. Willis, and M. El-Batanouny, Phys. Rev. B **40**, 2284 (1989).
[20] R. Boesch and C.R. Willis, Phys. Rev. B **39**, 361 (1989).
[21] N.J. Balmforth, R.C. Craster, and P.G. Kevrekidis, Physica D **135**, 212 (2000).
[22] C. Willis, M. El-Batanouny, and P. Stancioff, Phys. Rev. B **33**, 1904 (1986).
[23] P. Stancioff, C. Willis, M. El-Batanouny, and S. Burdick, Phys. Rev. B **33**, 1912 (1986).
[24] R. Boesch, P. Stancioff, and C.R. Willis, Phys. Rev. B **38**, 6713 (1988).
[25] C.R. Willis and R. Boesch, Phys. Rev. B **41**, 4570 (1990).
[26] R. Boesch and C.R. Willis, Phys. Rev. B **42**, 6371 (1990).
[27] O.M. Braun, Yu.S. Kivshar, and M. Peyrard, Phys. Rev. E **56**, 6050 (1997).
[28] Yu.S. Kivshar, D.E. Pelinovsky, T. Cretegny, and M. Peyrard, Phys. Rev. Lett. **80**, 5032 (1998).
[29] T. Kapitula and B. Sandstede (unpublished), available at http://www.math.unm.edu/ kapitula
[30] T. Kapitula and B. Sandstede (unpublished) available at http://www.math.unm.edu/ kapitula.
[31] A.R. Bishop, S.E. Trullinger, and J.A. Krumhansl, Physica D **1**, 1 (1980).
[32] R.L. Pego and M.I. Weinstein, Philos. Trans. R. Soc. London, Ser. A **340**, 47 (1992).
[33] T. Kapitula, SIAM (Soc. Ind. Appl. Math.) J. Math. Anal. **30**, 273 (1999).
[34] R.L. Pego and M.I. Weinstein, in *Mathematics in Science and Engineering*, edited by W.F. Ames, E.M. Harrell II, and J.V. Herod (Academic, Orlando, 1993), Vol. 192.
[35] S. Chow, J. Hale, and J. Mallet-Paret, J. Diff. Eqns. **37**, 351 (1980).
[36] J.P. Keener and D.W. McLaughlin, Phys. Rev. A **16**, 777 (1977).
[37] D.W. McLaughlin and A.C. Scott, Phys. Rev. A **18**, 1652 (1978).